



# Friction and wear behaviors of Nb–Ti–Si–Cr based ultrahigh temperature alloy and its Zr–Y jointly modified silicide coatings

Xuan LI, Xi-ping GUO, Yan-qiang QIAO

State Key Laboratory of Solidification Processing, Northwestern Polytechnical University, Xi'an 710072, China

Received 12 June 2015; accepted 11 December 2015

**Abstract:** Zr–Y jointly modified silicide coatings were prepared on an Nb–Ti–Si–Cr based ultrahigh temperature alloy by pack cementation process. The wear behaviors of both the base alloy and coatings were comparatively studied at room temperature and 800 °C using SiC balls as the counterpart. The Zr–Y jointly modified silicide coating is mainly composed of a thick (Nb,X)Si<sub>2</sub> outer layer and a thin (Ti,Nb)<sub>5</sub>Si<sub>4</sub> inner layer. The coatings possess much higher microhardness than the base alloy. The wear rates of both the base alloy and coatings increase with increasing the sliding loads. However, the coatings have much lower wear rates than the base alloy under the same sliding conditions. The coatings have superior anti-friction property, and can provide effective protection for the base alloy at both room temperature and 800 °C in air.

**Key words:** Nb–Ti–Si–Cr based alloy; Zr–Y modified silicide coating; friction and wear; wear mechanism

## 1 Introduction

Nb–Si based ultrahigh temperature alloys are attractive for structural applications due to their high melting point, good high-temperature strength and relatively low density [1,2]. Within such an alloy system, Nb solid solution (Nbss) offers room temperature ductility, and the silicides ( $\alpha$ ,  $\beta$ ,  $\gamma$ -Nb<sub>5</sub>Si<sub>3</sub> and/or Nb<sub>3</sub>Si) supply the strength and creep resistance at elevated temperatures, thereby leading to a good balance of low-temperature toughness and high-temperature strength [3,4]. However, the fracture and oxidation properties of these alloys are inadequate for high-temperature structural applications, which seriously impede their practical use [5]. The addition of alloy elements such as Ti, Cr, Mo, W, Hf and B has been proved to be an effective way to improve the high-temperature oxidation resistance and fracture toughness of Nb–Si based alloys [6–10]. Unfortunately, the improvement via single alloying method is still not enough to meet the requirements of practical applications of Nb–Si based alloys at high temperatures [6,11]. Moreover, the excessive addition of some alloying elements that are beneficial to the improvement in oxidation resistance would also impose deleterious

influences on the mechanical properties of the alloys [2,5]. Thus, a protective coating is necessary for the practical use of this type of alloys.

Niobium disilicide coatings are suitable for protecting Nb–Si based alloys from oxidation at high temperatures [12–14]. However, the brittleness of these coatings is a serious barrier to their long-term applications. Moreover, non-protective Nb<sub>2</sub>O<sub>5</sub> always forms in the scale during oxidation because the affinity of Nb for oxygen is relatively close to that of Si [12], which seriously weakens the high-temperature oxidation resistance of NbSi<sub>2</sub> coatings. Adding reactive elements such as Ge, Zr and Y is effective in improving the high-temperature oxidation resistance of NbSi<sub>2</sub> coating, as a result of the reactive element effects (REES) [15–18]. TIAN and GUO [16] found that the Y-modified silicide coatings have better oxidation resistance than the simple siliconized coating. Our previous studies [17,18] have also proved that the Zr–Y jointly modified silicide coating prepared on Nb–Ti–Si–Cr based ultrahigh temperature alloy possesses superior oxidation resistance to the pure silicide coating.

In addition to the high temperature oxidation resistance, the tribological properties are also important to high-temperature structural materials under the operating conditions, as wear can lead to serious

reduction on the lifetime of their service parts [19–21]. However, although the oxidation behavior of numerous Nb–Si based alloys and their protective silicide coatings has been studied in the open literature, as mentioned above, their wear properties were hardly mentioned and understood. The present study is the extension of our previous work reported on the development of oxidation resistant Zr–Y jointly modified silicide coating prepared on Nb–Ti–Si–Cr based ultrahigh temperature alloy [17,18]. In this study, the microhardness and the friction and wear behavior of Nb–Ti–Si–Cr based alloy and its Zr–Y jointly modified silicide coatings were comparatively investigated at room temperature and 800 °C, under different sliding loads. The wear mechanisms of the bare alloy and the coated specimens were also discussed on the basis of their wear track analysis.

## 2 Experimental

### 2.1 Preparation of wear specimens

The Nb–Ti–Si–Cr based alloy used for the wear tests and coating substrate has a nominal composition of 45Nb–29Ti–8Si–11Cr–4Hf–3Al (mole fraction, %), which was prepared by vacuum consumable arc-melting in argon atmosphere. Figure 1 shows the back scattered electron (BSE) image of the microstructure of the arc-melted alloy, and Table 1 lists the chemical compositions of its constituent phases. It can be seen that the microstructure of the arc-melted alloy mainly consists of primary Nbss, Nbss/(Nb, X)<sub>5</sub>Si<sub>3</sub> (X represents Ti, Cr and Hf elements) and Nbss/(Nb, X)<sub>5</sub>Si<sub>3</sub>/Cr<sub>2</sub>Nb eutectics.

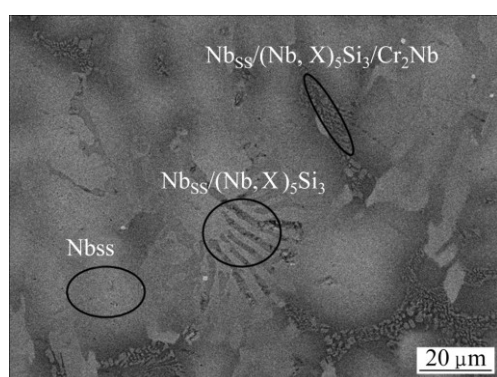


**Fig. 1** BSE image of arc-melted Nb–Ti–Si–Cr based ultrahigh temperature alloy

**Table 1** Compositions of constituent phases in Fig. 1 determined by EDS analyses

Phase	Mole fraction/%					
	Nb	Ti	Si	Cr	Al	Hf
Nbss	47.9	30.7	4.3	9.2	4.8	3.1
(Nb, X) <sub>5</sub> Si <sub>3</sub>	30.4	22.7	34.9	1.2	3.2	7.6
Cr <sub>2</sub> Nb	21.8	17.4	7.9	45.1	1.6	6.2

The Zr–Y jointly modified silicide coatings were prepared in a self-made high temperature and high vacuum cementation furnace. According to the results reported in Refs. [17,18], the coating was prepared at 1250 °C for 8 h using pack mixtures composed of 10Si–10Zr–3Y<sub>2</sub>O<sub>3</sub>–5NaF–72Al<sub>2</sub>O<sub>3</sub> (mass fraction, %). In the pack mixtures, Si, Zr and Y<sub>2</sub>O<sub>3</sub> powders were used as the depositing source, NaF as the activator and Al<sub>2</sub>O<sub>3</sub> as the inert filler. Before packing, the powders were mixed up by tumbling in a ball mill for 4 h. The detailed preparation processes of the coating can be found in Refs. [16–18].

### 2.2 Friction and wear tests

Friction and wear tests were conducted on an HT–1000 friction-wear testing machine by a ball-on-disc tribometer at room temperature and 800 °C. SiC balls with a diameter of 4.76 mm were chosen as the counterparts, as SiC is commonly used as components for thermal structure assemblies and wear resistant applications [22,23]. Considering that the base alloy and the coatings can only be used under small load conditions for applications on contact surfaces due to their fragility, relatively low sliding loads (3.234, 5.194 and 7.154 N) and velocity (0.094 m/s) were chosen for the tests. All the tests were performed for 60 min at a gyration radius of 4 mm, and at least two tests were undertaken for each condition for repeatability. Before and after wear tests, each specimen was weighed using an analytical balance (SHIMADZU, AUW220D) with an accuracy of 0.01 mg. For the sake of repeatability, an average value of 5 measured data was employed for each reported point.

### 2.3 Analysis and characterization methods

An HV–1000 Knoop microhardness tester with a Knoop indenter was employed to measure the microhardness of the base alloy and the coating, at a load of 0.245 N and loading time of 20 s. To take the repeatability into account, the reported hardness values were the average of 5 indentation readings. X-ray diffraction (XRD, Panalytical X'Pert PRO) was used to identify the phase constituents of the coating and the worn surfaces. Scanning electron microscopy (SEM, Zeiss Supra–55) equipped with an energy dispersive spectroscopy (EDS, Inca X-sight) was employed to identify the phase constituents, compositional distribution and structures of the base alloy and the coatings, including the worn surfaces generated in the wear tests.

## 3 Results

### 3.1 Structure of Zr–Y jointly modified silicide coating

Figure 2 shows the BSE images and the element

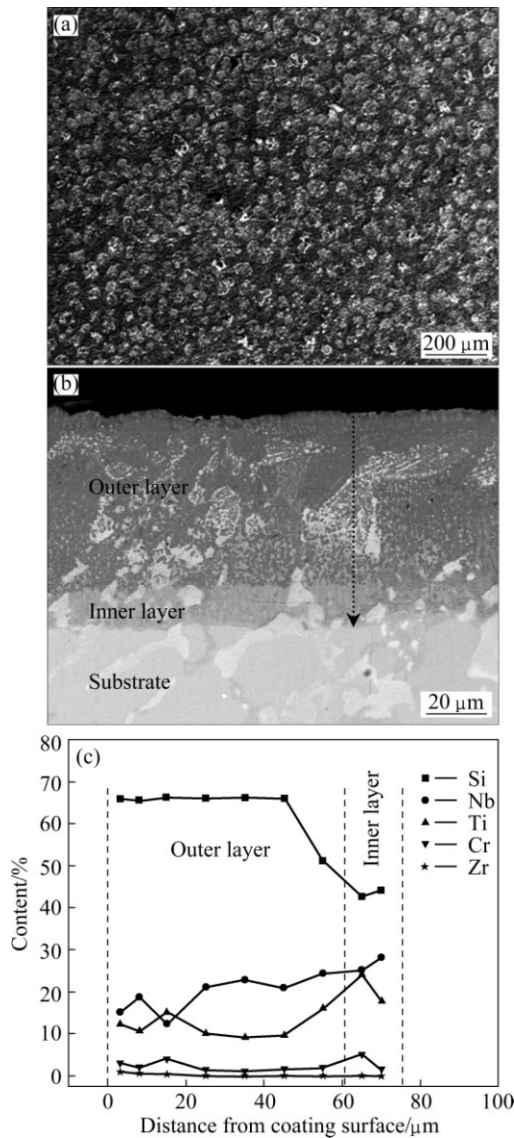


**Fig. 2** Surface (a) and cross-sectional (b) BSE images and element content profile (c) of Zr–Y jointly modified silicide coating prepared at 1250 °C for 8 h

content profile of the Zr–Y jointly modified silicide coating. From Fig. 2(a), it can be seen that the coating is relatively dense, and considerable asperities can be found on the coating surface. The cross-sectional BSE image of the coating (Fig. 2(b)) shows a double-layer structure: an outer layer with a thickness about 60 μm and an inner layer with a thickness about 15 μm. The EDS analysis results in Fig. 2(c) reveal that the outer layer is mainly composed of  $(\text{Nb}, \text{X})\text{Si}_2$  (X presents Ti, Cr, Hf and Zr elements) and the inner layer is mainly composed of  $(\text{Ti}, \text{Nb})_5\text{Si}_4$ . This is also verified by the XRD patterns conducted on the surface and inner layer of the coating (the XRD pattern of the inner layer is obtained by stripping off the coating about 65 μm from its original surface), as shown in Fig. 3. The light-grey phases in both outer and inner layers of the coating are rich in Hf

but poor in Si compared with the corresponding grey matrix, mainly because they are transformed from the primary  $(\text{Nb}, \text{X})_5\text{Si}_3$  in the base alloy [16]. In addition, such a multilayer coating structure could offer a composition gradient between the coating and substrate, which should be effective in suppressing the formation of micro-cracks in the coating during the cooling process and result in stronger coating/substrate bonding [24,25]. This would be beneficial to improving the wear resistance of the coating by preventing spallation during sliding.

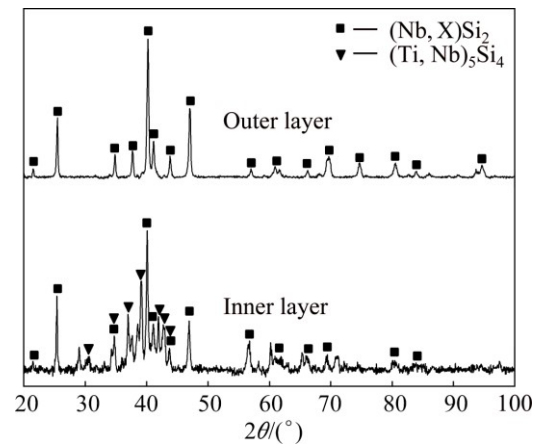


**Fig. 3** XRD patterns conducted on surface and inner layer of Zr–Y jointly modified silicide coating prepared at 1250 °C for 8 h

### 3.2 Microhardness of Zr–Y jointly modified silicide coating

Figure 4 presents the typical SEM image of Vickers indentation topography, as well as the microhardness distribution profile along the depth direction from the coating surface to the substrate. It is obvious that the coating possesses much higher microhardness than the base alloy: the microhardnesses of the  $(\text{Nb}, \text{X})\text{Si}_2$  outer layer and the  $(\text{Ti}, \text{Nb})_5\text{Si}_4$  inner layer are higher than  $\text{HV}_{0.245}$  1200 and  $\text{HV}_{0.245}$  900, respectively, while that of the base alloy is located in the range of  $\text{HV}_{0.245}$  (550–650). The microhardness differences should be associated with different contents of Si, i.e., a higher Si content would lead to higher microhardness. Since the wear resistance of a certain material is mainly related to its surface hardness [26,27], the Zr–Y jointly modified silicide coating would possess higher wear resistance. Additionally, cracks are hardly observed in the coating and coating/substrate interface even after the microhardness tests, which indicates that the bonding quality between the coating and the substrate is relatively good.

### 3.3 Friction coefficients and wear rates

Figures 5(a)–(c) illustrate the variation of friction

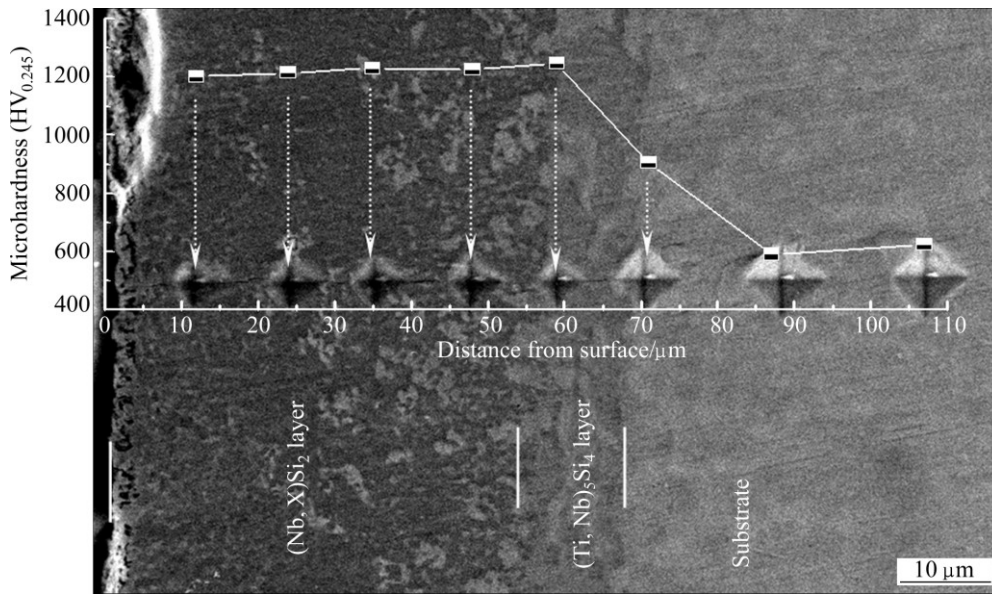


Fig. 4 SEM image of Vickers indentation topography and microhardness distribution profile from coating surface to substrate

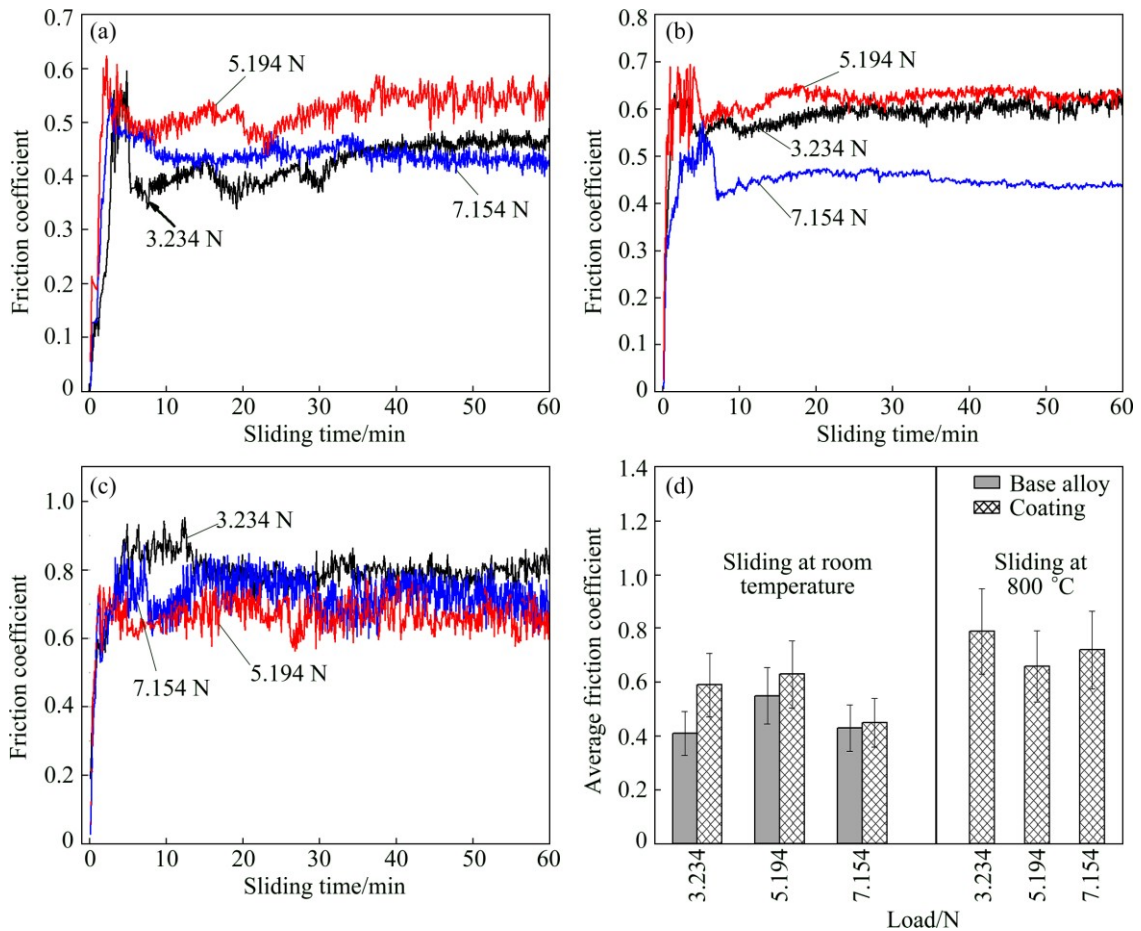


Fig. 5 Friction coefficients of base alloy sliding at room temperature (a) and coating sliding at room temperature (b) and 800 °C (c) under sliding loads of 3.234, 5.194 and 7.154 N, and average friction coefficients under sliding conditions of (a–c) (d)

coefficients as a function of sliding time for both base alloy and coated specimens sliding at room temperature and 800 °C with a velocity of 0.094 m/s, under the loads of 3.234, 5.194 and 7.154 N. Figure 5(d) presents the

average friction coefficients for the base alloy and the coating under the applied sliding conditions in Figs. 5(a)–(c). The friction coefficients of the base alloy sliding at 800 °C are not presented because catastrophic

failure occurred on its worn surfaces during sliding, as a result of its rather poor oxidation resistance [1,6]. It is obvious that although a number of alloying elements such as Ti, Cr, Hf and Al have been added in the base alloy to improve its oxidation resistance, the improvement via single alloying modification is not enough to meet the requirements for sliding at high temperatures.

As can be seen from Fig. 5, the friction coefficients of both base alloy and coating increase rapidly in the initial sliding stage and then reach steady state due to the wear of asperities and the formation of wear debris. For the base alloy sliding at room temperature, as shown in Figs. 5(a) and (d), the average friction coefficient of the base alloy increases from about 0.41 to 0.55 with increasing the sliding load from 3.234 to 5.194 N; however, increasing the load to 7.154 N results in the decrease of average friction coefficient to 0.43. Similar trend is observed for the coating sliding at room temperature (Figs. 5(b) and (d)): the average friction coefficient of the coating increases from about 0.59 to 0.63 with increasing the sliding loads from 3.234 to 5.194 N, and then decreases to 0.42 with increasing the sliding load to 7.154 N. When the sliding temperature increases to 800 °C, as shown in Figs. 5(c) and (d), the friction coefficients of the coatings become oscillated. Moreover, the average friction coefficients of the coatings are higher than those of the base alloy sliding at room temperature under the same sliding loads.

Figure 6 compares the variation characteristics of the wear rates of the specimens with and without coating at room temperature and 800 °C for 60 min, under the sliding loads of 3.234, 5.194 and 7.154 N. The specific wear rates for the base alloy and the coatings are calculated using the following equation [23]:

$$W=2\pi rA/(FL) \quad (1)$$

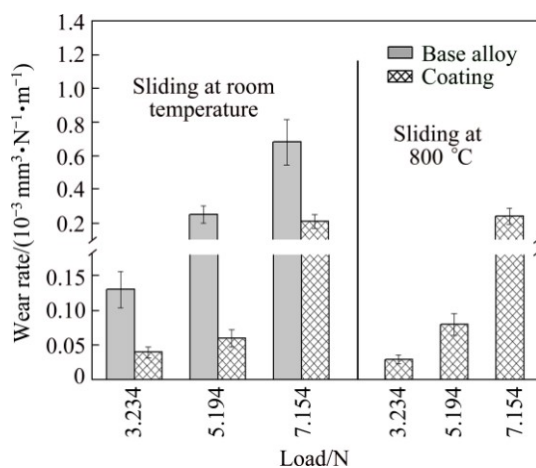


**Fig. 6** Wear rates of base alloy and coating sliding at room temperature and 800 °C for 60 min, under loads of 3.234, 5.194 and 7.154 N

where  $r$  is the disk wear track radius,  $A$  is the cross-sectional area of the wear track,  $F$  is the normal load and  $L$  is the sliding distance. It is obvious that the coating sliding at room temperature shows considerably lower wear rates than the base alloy under the same sliding loads. It is clear that Zr–Y jointly modified silicide coating possesses much better anti-friction performance at both room temperature and 800 °C, as catastrophic failure occurs on the worn surfaces of the base alloy sliding at 800 °C. This should be partially resulted from the enhancement in surface microhardness and better high temperature oxidation resistance of the Zr–Y jointly modified silicide coating [6].

From Fig. 6, it can also be seen that the wear rates of both base alloy and the coating display an increase tendency with the increase of sliding loads, irrespective of the sliding temperatures. This reveals that larger sliding loads would impose more serious wear on both base alloy and coatings under the applied conditions. In most cases, the coatings sliding at 800 °C have larger wear rates than those sliding at room temperature, suggesting that sliding temperature also plays an accelerative role in the wear rates of the coating. Specially, under lower sliding load of 3.234 N, the wear rate of the coating sliding at 800 °C is a little lower than that of the coating sliding at room temperature. Such a reduction should be associated with the rapid formation of oxidation products between the friction pairs at a higher temperature, and this will be discussed later.

### 3.4 Wear morphologies

In order to further understand the wear behavior of the base alloy and the coating, the SEM images of the typical worn surfaces of the specimens as well as their SiC counterparts are chosen for analysis, as shown in Figs. 7–9. Meanwhile, the EDS and microzone XRD analyses of the worn surfaces were also carried out to supply auxiliary information for determining the wear mechanisms, and the results are presented in Tables 2–4 and Fig. 10, respectively. From Figs. 7 and 8, it can be seen that the wear track of the Zr–Y jointly modified silicide coating is much smaller and narrower than that of the base alloy under the applied conditions. With increasing the sliding temperature to 800 °C, the wear track of the coating becomes larger and smoother, as shown in Fig. 9.

As can be seen from Figs. 7(a) and (b), the worn surface of the base alloy is rather rough, where the surface damages such as serious plastic deformation and adhesive craters could be clearly observed. It is obvious that the SiC ball causes serious wear on the base alloy. The worn zone of the base alloy is characterized by black (point 1) and grey areas (point 2). The EDS analysis demonstrates that abundant oxygen exists in the black

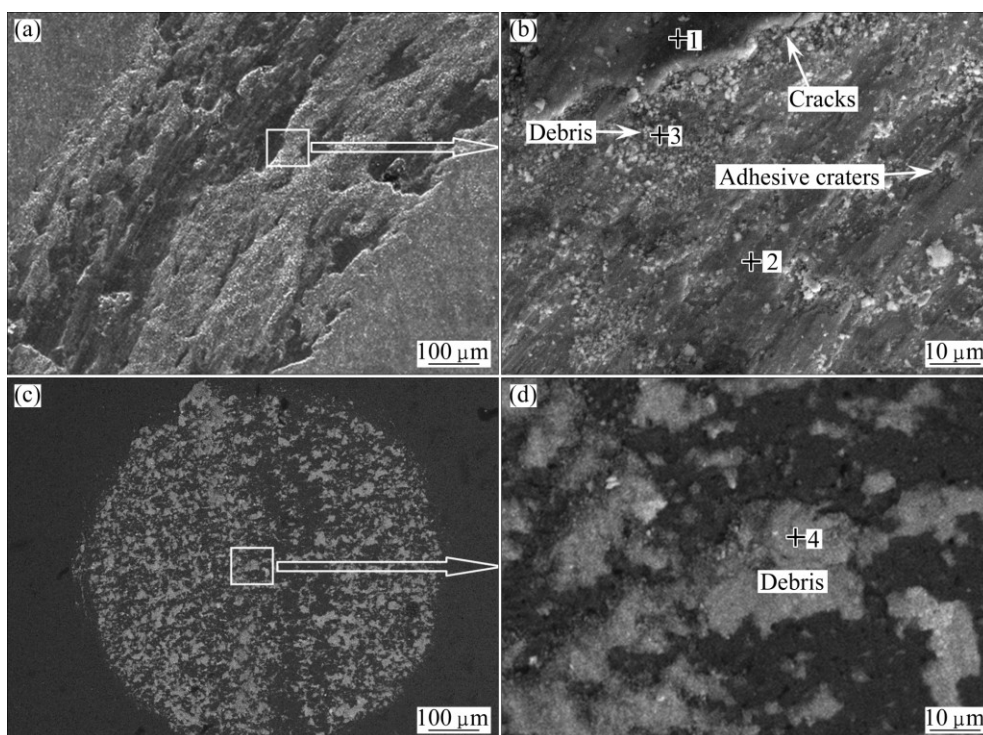


**Fig. 7** Wear morphologies of base alloy (a, b) and SiC counterpart (c, d) after sliding at room temperature for 60 min under load of 5.194 N

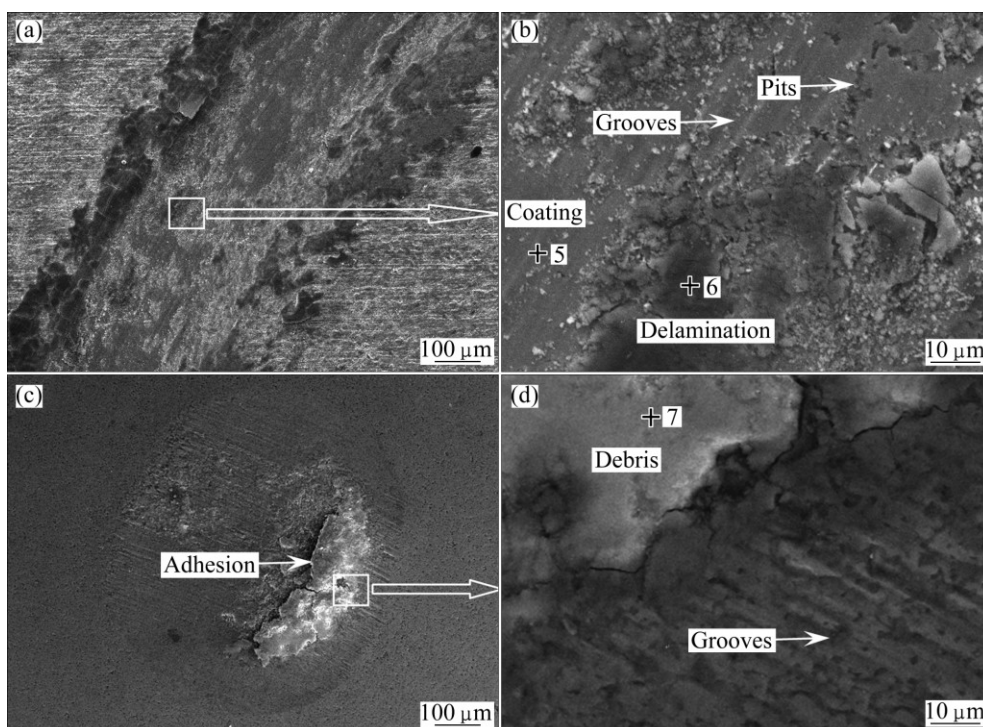


**Fig. 8** Wear morphologies of Zr–Y jointly modified silicide coating (a, b) and SiC counterpart (c, d) after sliding at room temperature for 60 min under load of 5.194 N

areas. Moreover, higher magnified image in Fig. 7(b) highlights that there are many fine debris with oxygen content of about 66.0% (mole fraction) (point 3) located in the wear track. The microzone XRD pattern conducted

on the wear track also shows the diffraction peaks of  $\text{SiO}_2$  and  $\text{Ti}_2\text{Nb}_{10}\text{O}_{29}$ , as can be seen from Fig. 10. The above observations clearly demonstrate the occurrence of oxidation on the worn surface of the base alloy.

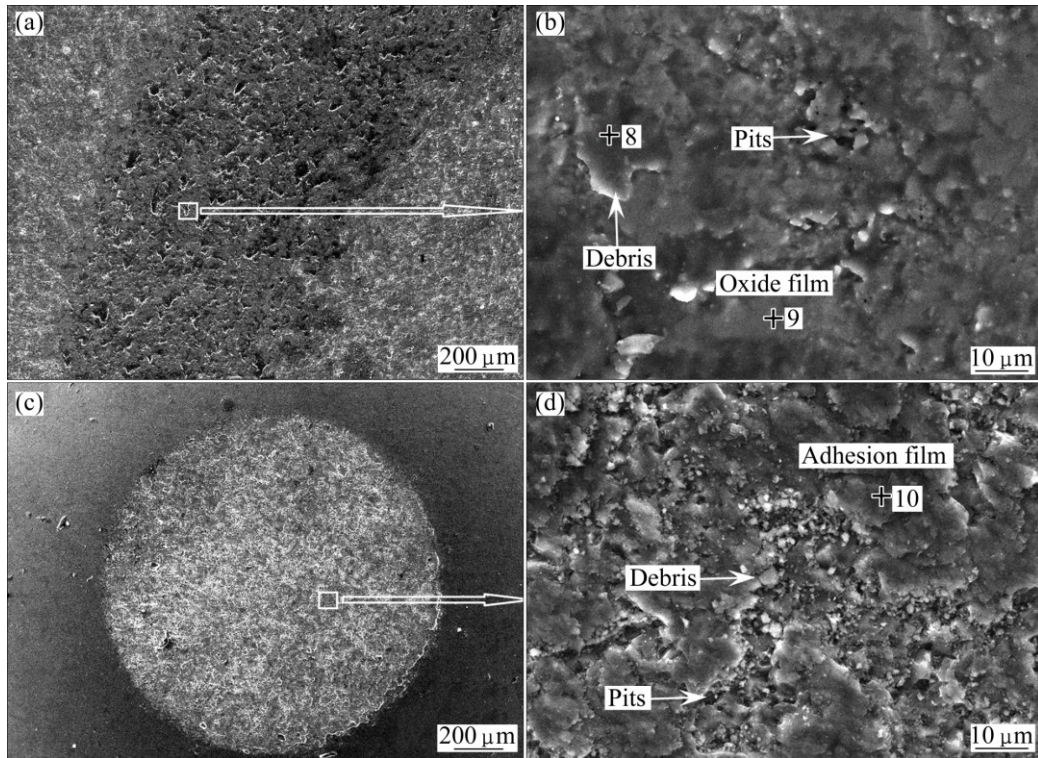


**Fig. 9** Wear morphologies of Zr–Y jointly modified silicide coating (a, b) and SiC counterpart (c, d) after sliding at 800 °C for 60 min under load of 5.194 N

**Table 2** Compositions of phases marked by plus symbols with numerals “1–4” in Fig. 7, determined by EDS analyses

Site	Mole fraction/%						
	Nb	Si	Ti	Cr	Al	Hf	O
1	16.1	8.8	10.7	2.9	1.5	1.8	58.2
2	30.3	11.4	24.8	5.8	2.8	4.0	20.9
3	13.6	7.4	8.3	2.0	1.3	1.4	66.0
4	13.1	16.6	11.6	4.4	1.5	1.4	51.4

**Table 3** Compositions of phases marked by plus symbols with numerals “5–7” in Fig. 8, determined by EDS analyses

Site	Mole fraction/%				
	Nb	Si	Ti	Cr	O
5	22.4	63.2	12.1	2.3	–
6	6.1	21.2	4.4	1.0	67.3
7	5.2	22.3	9.6	3.6	59.3

**Table 4** Compositions of phases marked by plus symbols with numerals “8–10” in Fig. 9, determined by EDS analyses

Site	Mole fraction/%				
	Nb	Si	Ti	Cr	O
8	2.5	29.6	2.3	0.7	64.9
9	6.6	27.9	6.0	1.1	58.4
10	2.0	47.0	1.5	0.6	48.9

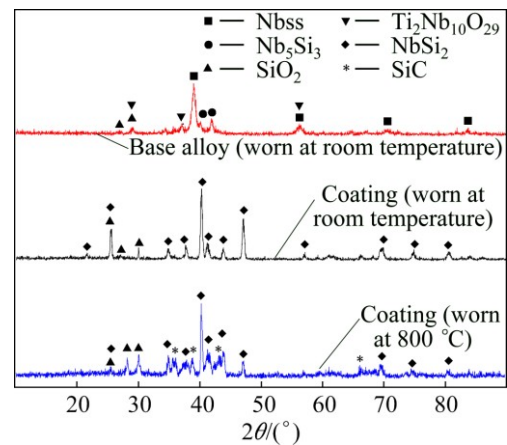


**Fig. 10** Microzone XRD patterns conducted on worn surfaces of base alloy and Zr–Y jointly modified silicide coatings after sliding for 60 min under load of 5.194 N

The wear zone of the SiC ball against the base alloy is shown in Figs. 7(c) and (d). The adhesions of the wear debris could be obviously observed on the worn surface. The EDS analysis (point 3) reveals that these adhesions are the outcomes of the oxidized Nbss, which suggests that adhesion and oxidation are prone to occur in Nbss phase of the base alloy due to its lower hardness [23]. With respect to the results of SEM, EDS and microzone XRD analyses, the most involved wear mechanism of the base alloy at room temperature could be concluded as

severe plastic deformation associated with oxidation wear and adhesive wear, accompanied with minor abrasive wear.

The Zr–Y jointly modified silicide coating displays different wear track morphologies (Figs. 8(a) and (b)), as severe delamination instead of plastic deformation could be clearly observed on its worn surface. Moreover, the asperities on the coating surface are eliminated, and many shallow grooves and pits appear in the wear track. The above factors reveal the delamination wear. The worn surface is mainly characterized by two distinct sections: one section should be the remained coating areas (point 5) that have a similar chemical composition to the original surface of the coating. This proves that the coating did not lose its effectiveness after sliding under the applied conditions in Fig. 8, suggesting the relatively good wear resistance of the Zr–Y jointly modified silicide coating. Another section is the delaminations with a mass of wear debris dispersed around them, as marked by point 6 in Fig. 8(b). The EDS analysis reveals that these delaminations have a typical composition of 6.1Nb–21.2Si–4.4Ti–1.0Cr–67.3O (mole fraction, %), implying the formation of  $\text{SiO}_2$ . This is also confirmed by the microzone XRD pattern conducted on the worn surface, as shown in Fig. 10.

It can be seen from Figs. 8(c) and (b) that there are intensive debris and grooves on the worn surface of the SiC ball. The EDS analysis reveals that these adhesions (point 7) possess relatively high contents of Nb, Ti, Cr and O, indicating that they are outcomes of the Zr–Y jointly modified silicide coating. The above factors demonstrate that the coating and its SiC counterpart create strong plough to each other. Thus, based on the above observations, it is allowed to draw a conclusion that the wear mechanism of Zr–Y jointly modified silicide coating could be dominated by delamination wear and abrasion wear.

Figure 9 presents the SEM images of the worn surfaces of the Zr–Y jointly modified silicide coating and the SiC counterpart after sliding at 800 °C for 60 min, under the same sliding load of 5.194 N as applied in Figs. 7 and 8. From Figs. 9(a) and (b), it can be seen that the wear track is wider but smoother than that of the coating sliding at room temperature (Fig. 8). However, it seems that serious adhesive wear occurs because many adhesive craters and wear debris can be found on the worn surface. In addition, the EDS analysis results in Table 4 and the microzone XRD pattern conducted on the worn surface (Fig. 10) indicate that  $\text{SiO}_2$  forms in the wear track of the coating.

The worn surface of the SiC ball sliding against the coating at 800 °C is much larger than that sliding at room temperature, as shown in Fig. 9(b). Moreover, the microzone XRD pattern in Fig. 10 shows relatively

strong intensity of the diffraction peaks of SiC. The above observations demonstrate that the coating creates serious wear on its SiC ball when sliding at 800 °C. The higher magnified image in Fig. 9(d) reveals that the worn zone of the SiC ball is covered by adhesion film. The EDS analysis demonstrates that significant quantities of O, Nb, Ti and Cr can be detected in this film, demonstrating that it is the outcomes of the oxidized coating. On the basis of the above analysis, the most involved wear mechanisms of the Zr–Y jointly modified silicide coating sliding at 800 °C can be considered as severe oxidation wear and adhesive wear.

## 4 Discussion

Lower microhardness of the base alloy makes plastic deformation occur on its worn surface during sliding. This would produce large friction energy at the contact point and subsequently cause oxidation, as plastic deformation would make adhesive wear increase [28,29]. Moreover, higher sliding load would aggravate the plastic deformation between the friction pairs and result in more serious oxidation by producing more friction energy. Thus, the wear rates of the base alloy increase with the increase of sliding load, as shown in Fig. 6. It should be emphasized that the adhesive junction between the friction pairs could be relatively strong. Thus, the broken of the adhesive junction would create adhesive craters on the worn surface, as shown in Fig. 7. With the sliding proceeding, the micro-cracks in the near surface of the worn zone generate, expand, and subsequently translate to fatigue cracks. As a result, the worn zone could not maintain its integrity and be gradually removed from the coating surface with the fatigue crack propagation. A part of the spallation products would get rid of the worn surfaces, causing wear loss, while some of them would engage in the friction and be gradually ground into small abrasive particles, and subsequently, create abrasive wear.

The high microhardness and strong coating/base alloy bonding make that Zr–Y jointly modified silicide coating possesses relatively good resistance to plastic deformation, which would in turn lower the wear rate [23]. However, under the shear action, the upper parts of the coating including the asperities on the coating surfaces would be gradually removed due to their brittleness, and the pits on the worn surfaces would be left, as can be seen from Fig. 8. This mechanism of material removal would become more intensified with the increase of sliding load, and lead to a larger wear rate, as shown in Fig. 6. The delaminations generated on the worn surfaces would be involved in the friction, and some of them were subsequently rolled into fine particles. These fine particles can plough the coating just like

abrasive grains, leading to abrasive wear. Moreover, the delaminations and debris can be oxidized cumulatively as a result of the friction heat. Such oxidation products (mainly composed of  $\text{SiO}_2$ ) are considered to be favorable for improving the wear resistance, by partially preventing the direct contact of the coating and the counterpart, and this should be one of the main factors that makes the coating possess superior wear resistance to the base alloy [30].

When sliding at 800 °C, a dense and fluxible  $\text{SiO}_2$  film forms on the worn surfaces of the Zr–Y jointly modified silicide coating, owing to the high sliding temperature and sufficient oxygen on the worn surfaces. The  $\text{SiO}_2$  film can act as a lubricating cover and protect the coating from further damage [23]. This makes the Zr–Y jointly modified silicide coating possess relatively good wear resistance at high temperature (800 °C). Such a protection mechanism can also explain why the coatings sliding at 800 °C with the load of 3.234 N even possess lower wear rate than the coating sliding at room temperature (Fig. 6): higher sliding temperature causes the rapid formation of protective  $\text{SiO}_2$  film between the friction pairs, and prevents the worn surface from further damage later. However,  $\text{SiO}_2$  film is soft in nature at high temperatures and has certain plastic deformation capacity, which would cause adhesive wear, evidenced by intensive pits on the worn surface shown in Fig. 9(b). Such an adhesive wear mechanism would lead to a higher friction coefficient as the adhesive junction between the friction pairs could be relatively strong. Thus, the friction coefficients of the coating sliding at room temperature are higher than those sliding at 800 °C under the same sliding loads, as shown in Fig. 5(d). It is also believed that higher sliding loads would aggravate adhesive wear on the worn surfaces, and cause a larger wear rate, as demonstrated in Fig. 6.

## 5 Conclusions

1) The Zr–Y jointly modified silicide coating has a double-layer structure, consisting of a thick  $(\text{Nb}, \text{X})\text{Si}_2$  outer layer and a thin  $(\text{Ti}, \text{Nb})_5\text{Si}_4$  inner layer. The coating possesses much higher microhardness than the base alloy.

2) The wear rates of both the base alloy and coating show an increase tendency with the increase of sliding loads, irrespective of the sliding temperatures.

3) The Zr–Y jointly modified silicide coating possesses better anti-friction property than the base alloy. Sliding at room temperature, the coating possesses much lower wear rates than the based alloy under the same sliding loads. Sliding at 800 °C, the coating is still protective after sliding for 60 min under the applied conditions, however, catastrophic failure occurs on the

worn surfaces of the base alloy.

4) At room temperature, the wear mechanisms of the base alloy can be concluded as severe plastic deformation associated with oxidation wear and abrasive wear, and minor abrasive wear, while the wear mechanisms of the coating are supposed to be delamination wear and abrasion wear. At 800 °C, the wear mechanisms of coating could be severe oxidation wear and adhesive wear.

## References

- [1] BEWLAY B P, JACKSON M R, ZHAO J C, SUBRAMANIAN P R. A review of very-high temperature Nb–silicide-based composites [J]. *Metallurgical and Materials Transactions A*, 2003, 34(10): 2043–2052.
- [2] PINT B A, DISTEFANO J R, WRIGHT I G. Oxidation resistance: One barrier to moving beyond Ni-base superalloys [J]. *Metallurgical and Materials Transactions A*, 2006, 415(1–2): 255–263.
- [3] KIM W Y, TANAKA H, KASAMA A, HANADA S. Microstructure and room temperature fracture toughness of Nbss/Nb<sub>5</sub>Si<sub>3</sub> in situ composites [J]. *Intermetallics*, 2001, 9(9): 827–834.
- [4] CHAN K S. The fracture toughness of niobium-based in situ composites [J]. *Metallurgical and Materials Transactions A*, 1996, 27(9): 2518–2531.
- [5] MURAYAMA Y, HANADA S. High temperature strength, fracture toughness and oxidation resistance of Nb–Si–Al–Ti multiphase alloys [J]. *Science and Technology of Advanced Materials*, 2002, 3(2): 145–156.
- [6] MATHIEU S, KNITTEL S, BERTHOD P, MATHIEU S, VILASI M. On the oxidation mechanism of niobium-base in situ composites [J]. *Corrosion Science*, 2012, 60: 181–192.
- [7] ZELENITSAS K, TSAKIROPOULOS P. Effect of Al, Cr and Ta additions on the oxidation behaviour of Nb–Ti–Si in situ composites at 800 °C [J]. *Materials Science and Engineering A*, 2006, 416(1–2): 269–280.
- [8] CHAN K S. Alloying effects on fracture mechanisms in Nb-based intermetallic in-situ composites [J]. *Materials Science and Engineering A*, 2002, 329–331: 513–522.
- [9] VAZQUEZ A, VARMA S K. High-temperature oxidation behavior of Nb–Si–Cr alloys with Hf additions [J]. *Journal of Alloys and Compounds*, 2011: 509(25): 7027–7033.
- [10] SHA J B, HIRAI H S, TABARU T, KITAHARA A, UENO H S, HANADA S J. High-temperature strength and room-temperature toughness of Nb–W–Si–B alloys prepared by arc-melting [J]. *Materials Science and Engineering A*, 2004, 364(1–2): 151–158.
- [11] QIAO Yan-qiang, GUO Xi-ping, LI Xuan. Hot corrosion behavior of silicide coating on an Nb–Ti–Si based ultrahigh temperature alloy [J]. *Corrosion Science*, 2015, 91: 75–85.
- [12] VILASI M, STEINMETZ J, ALLEMAND B G. Protective coatings for niobium alloys [J]. *Journal of Advanced Materials*, 2000, 32: 53–57.
- [13] SUZUKI R O, ISHIKAWA M, ONO K. NbSi<sub>2</sub> coating on niobium using molten salt [J]. *Journal of Alloys and Compounds*, 2002, 336(1–2): 280–285.
- [14] QIAO Yan-qiang, GUO Xi-ping. Microstructures of Si–Cr co-depositing coatings prepared on Ti–Nb–Si based ultrahigh temperature alloy [J]. *The Chinese Journal of Nonferrous Metals*, 2009, 19(11): 1993–1999. (in Chinese)
- [15] WANG Wan, YUAN Bi-fei, ZHOU Chun-gen. Formation and oxidation resistance of germanium modified silicide coating on Nb based in situ composites [J]. *Corrosion Science*, 2014, 80: 164–168.

- [16] TIAN Xiao-dong, GUO Xi-ping. Structure and oxidation behavior of Si–Y co-deposition coatings on an Nb silicide based ultrahigh temperature alloy prepared by pack cementation technique [J]. Surface and Coatings Technology, 2009, 204(3): 313–318.
- [17] LI Xuan, GUO Xi-ping. Effects of activators on formation of Si–Zr–Y co-deposition coatings on Nb–Ti–Si–Cr based ultrahigh temperature alloy [J]. Acta Metallurgica Sinica, 2012, 48(11): 1394–1402.
- [18] LI Xuan, GUO Xi-ping, QIAO Yan-qiang. Structure and oxidation behavior of Zr–Y modified silicide coatings prepared on an Nb–Ti–Si–Cr based ultrahigh temperature alloy [J]. Oxidation of Metals, 2015, 83(3–4): 253–271.
- [19] JIN Pei-peng, CHEN Geng, HAN Li, WANG Jin-hui. Dry sliding friction and wear behaviors of Mg<sub>2</sub>B<sub>2</sub>O<sub>5</sub> whisker reinforced 6061Al matrix composites [J]. Transactions of Nonferrous Metals Society of China, 2014, 24(1): 49–57.
- [20] ZHANG Zhen-yu, LU Xin-chun, HAN Bao-lei, LUO Jian-bin. Rare earth effect on the microstructure and wear resistance of Ni-based coatings [J]. Materials Science and Engineering A, 2007, 454(25): 194–202.
- [21] HAJIALI FINI M, AMADEH A. Improvement of wear and corrosion resistance of AZ91 magnesium alloy by applying Ni–SiC nanocomposite coating via pulse electrodeposition [J]. Transactions of Nonferrous Metals Society of China, 2013, 23(10): 2914–2922.
- [22] CHEN Zi-shan, LI He-jun, FU Qian-gang, CHU Yan-hui, WANG Shao-long, HE Zi-bo. Tribological behavior of SiC coating on C/C composites against SiC and WC under unlubricated sliding [J]. Ceramics International, 2013, 39(2): 1765–1773.
- [23] CHEN Zi-shan, LI He-jun, FU Qian-gang. SiC wear resistance coating with added Ni, for carbon/carbon composites [J]. Surface and Coatings Technology, 2012, 213: 207–215.
- [24] ANASYIDA A S, DAUD A R, GHAZAL M J. Dry sliding wear behavior of Al–12Si–4Mg alloy with cerium addition [J]. Materials and Design, 2010, 31(1): 365–374.
- [25] XIANG Z D, ROSE S, DATTA P K. Pack deposition of coherent aluminide coatings on  $\gamma$ -TiAl for enhancing its high temperature oxidation resistance [J]. Surface and Coatings Technology, 2002, 161(2–3): 286–292.
- [26] RAJINIKANTH V, VENKATESWARLU K. An investigation of sliding wear behavior of WC–Co coating [J]. Tribology International, 2011, 44(12): 1711–1719.
- [27] GUO Hai-sheng, GUO Xi-ping. Microstructure and micro-hardness of directionally solidified and heat-treated Nb–Ti–Si based ultrahigh temperature alloy [J]. Transactions of Nonferrous Metals Society of China, 2011, 21(6): 1283–1290.
- [28] SHARMA S P, DWIVEDI D K, JAIN P K. Effect of La<sub>2</sub>O<sub>3</sub> addition on the microstructure, hardness and abrasive wear behavior of flame sprayed Ni based coatings [J]. Wear, 2009, 267(5–8): 853–859.
- [29] JONES L C, LLEWELLYN R J. Sliding abrasion resistance assessment of metallic materials for elevated temperature mineral processing conditions [J]. Wear, 2009, 267(11): 2010–2017.
- [30] KESHRI A K, AGARWAL A. Wear behavior of plasma-sprayed carbon nanotube reinforced aluminum oxide coating in marine and high-temperature environments [J]. Journal of Thermal Spray Technology, 2011, 20(6): 1217–1230.

## Nb–Ti–Si–Cr 基超高温合金及其 表面 Zr–Y 联合改性硅化物渗层的摩擦磨损性能

李 轩, 郭喜平, 乔彦强

西北工业大学 凝固技术国家重点实验室, 西安 710072

**摘 要:** 采用扩散共渗方法在 Nb–Ti–Si–Cr 基超高温合金表面制备 Zr–Y 改性的硅化物渗层, 对比研究基体合金和共渗层在室温和 800 °C 与 SiC 球对磨时的摩擦磨损性能。所制备的 Zr–Y 改性硅化物渗层主要由较厚的(Nb, X)Si<sub>2</sub> 外层和较薄的(Ti, Nb)<sub>5</sub>Si<sub>4</sub> 内层组成。共渗层的显微硬度明显高于基体合金。基体合金和共渗层在常温和 800 °C 时的磨损率均随摩擦载荷的增加而增加, 但在相同的摩擦条件下, 共渗层的磨损率明显低于基体合金。Zr–Y 改性硅化物渗层在室温和 800 °C 时的磨损抗力均优于基体合金, 能够为基体合金提供良好的保护。

**关键词:** Nb–Ti–Si–Cr 基合金; Zr–Y 改性硅化物渗层; 摩擦磨损; 磨损机制

(Edited by Mu-lan QIN)